

Metagenomics Disentangles Differential Resistome Traits and Risks in Full-Scale Anaerobic Digestion Plants under Ambient, Mesophilic, and Thermophilic Conditions

Published as part of ACS Environmental Au special issue “2024 Rising Stars in Environmental Research”.

Xinyu Zhu, Irini Angelidaki, Tong Zhang, and Feng Ju*



Cite This: ACS Environ. Au 2025, 5, 183–196



Read Online

ACCESS |

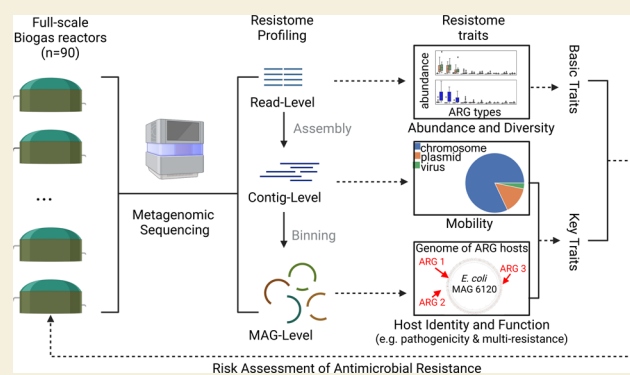
Metrics & More

Article Recommendations

Supporting Information

ABSTRACT: Anaerobic digestion (AD) systems are vital for converting organic waste to green bioenergy but also serve as a non-negligible environmental reservoir for antibiotic-resistance genes (ARGs) and resistant bacteria of environmental and human health concerns. This study profiles the antibiotic resistome of 90 full-scale biogas reactors and reveals that AD microbiomes harbor at least 30 types and 1257 subtypes of ARGs, of which 16% are located on plasmids showing potential mobility. The total abundance of AD-ARGs ranges widely from 0.13 to 7.81 copies per cell and is distributed into 42–739 subtypes, significantly influenced ($P < 0.05$) by operational conditions like digestion temperature and substrate types. Compared with the ambient and mesophilic digesters, the thermophilic digesters harbor a significantly lower abundance and diversity as well as greatly reduced mobility and host pathogenicity levels (all $P < 0.05$) of ARGs, revealing that a higher digestion temperature mitigates the overall resistome risks. The comprehensive analysis of basic traits and key traits of the AD resistome is demonstrated to provide crucial quantitative and qualitative insights into the diversity, distribution pattern, and health risks of ARGs in full-scale AD systems. The revealed knowledge offers new guidance for improving environmental resistome management and developing oriented mitigation strategies to minimize the unwanted spread of clinically important antimicrobial resistance from AD systems.

KEYWORDS: anaerobic digestion, antibiotic resistance gene, resistome, risk assessment, full-scale biogas digesters



1. INTRODUCTION

Anaerobic digestion (AD) is a broadly used applied green technology for harvesting renewable energy from various organic wastes, such as livestock manure, food wastes, agricultural residues, and wastewater sludge. The digestate generated from the AD processes contains high concentrations of nutrient elements (i.e., N, P, and K) and is often applied as a biofertilizer in agriculture. Using an AD effluent as biofertilizers has been proved to significantly improve soil physicochemical properties and promote plant growth.¹ However, the direct land application of AD digestates may lead to well-known environmental issues, such as the emission of greenhouse gases, nutrient leaching, and the spread of pathogens and micropollutants. Notably, the potential risks of spreading antimicrobial resistance (AMR) through digestate land utilization became a heated debate.^{2,3} The AD systems are widely used to valorize waste streams from human origins and animal farming activities; therefore, they are tightly connected to all major elements under One Health which recognizes that the health of humans, animals, and ecosystems are

interconnected. It is widely accepted that AMR is an increasing severe global public health concern, and it has affected human health due to its detrimental role within clinical settings.⁴ Moreover, the AMR has recently been highlighted as not simply a problem within healthcare facilities because various pristine environments and engineering infrastructures contribute to the emergence, acquisition, and spread of AMR.^{5,6}

The AMR is usually genetically encoded and occurs through overexpression or duplication of existing genes, point mutations, or the acquisition of entirely new genes via horizontal gene transfer. Many mega-studies, which investigated animal or environmental resistome, i.e., the collection

Received: July 31, 2024

Revised: November 7, 2024

Accepted: November 7, 2024

Published: December 5, 2024



of antibiotic resistance genes (ARGs), on a broad geographical or temporal scale, have been conducted to unveil the distribution and dissemination potential of ARGs using sequencing-based methods, covering nearly all habitats, including guts,^{7,8} soil,^{9,10} marine,¹¹ freshwater,¹² built-environment,¹³ and wastewater treatment plants.^{14,15} Different from these mega studies, AD-ARG research primarily focuses on the ARG removal during the digestion processes as well as the practical mitigation measures that enhance the elimination of ARG.³ Antibiotic exposure is one of the most important drivers for ARG enrichment and dissemination in AD systems.^{16–19} In addition, operational parameters, such as temperature,^{20,21} substrate types,²² and ammonia levels,²³ have been also proved to affect the fate of specific ARGs in AD systems. To further control the health risks of AD-ARGs, various additives have been shown to facilitate ARG removal with promising results, including biochars,^{24,25} copper,²⁶ zerovalent iron,²⁷ iron nanoparticles,²⁸ and carbon materials.²⁹ However, most AD-ARG research focused on small-scale experimental setups and specific ARGs (only a subset of resistome) in individual biogas reactors. A global overview of AD-ARG in full-scale AD infrastructures is an unmet need to guide resistome risk assessment as well as the development of mitigation strategies.

Conventionally, AMR has been widely concerned in the human microbiome, relating to the insufficient or failed control on pathogenic bacterial infections. However, realizing the importance of environmental reservoirs in combating AMR under the One Health approach has launched extensive studies on the environmental dimensions (e.g., fate, evolution, and spread) of antibiotic resistance.^{4,30} The ultrahigh diversity of environmental microbiomes (e.g., at least thousands of species in 1 mg soil or 1 mL activated sludge)¹⁵ and difficulties in microbial cultivation hinder classic phenotypic identification of AMR. Luckily, recent advancements of high-throughput sequencing-based metagenomic methods and bioinformatics resources have significantly enhanced our abilities to detect and study AMR in various environmental and human microbiomes.^{8,13,31–34} The metagenomics-based resistome characterization is typically performed on three levels: (1) reads level, where the short reads generated from high-throughput sequencing platforms (e.g., Illumina HiSeq or NovaSeq) are directly aligned or mapped to reference sequences in an ARG database (e.g., CARD³⁵ and SARG³⁶) to identify ARG-like reads, (2) contig level, where the metagenomic reads are de novo assembled to generate longer contigs whose open reading frames (ORFs) are further predicted and searched against an ARG database, and (3) genome level, where the contigs are binned into metagenomic-assembled genomes (MAGs) so that the host taxonomy and functional potential of ARGs could be precisely identified and further evaluated.

In the current study, we systematically characterized the antibiotic resistome of 90 full-scale biogas reactors³⁷ with complementary metagenomic strategies on reads, contigs, and genome level. The results reveal both quantitative basic traits (i.e., ARG diversity and abundance) and qualitative key traits (e.g., mobility and host pathogenicity) of the AD resistome. The comparison of the resistome characteristics among ambient, mesophilic, and thermophilic digesters leads to an in-depth discussion on and insights into how operational temperature affects the spread and mitigation of ARGs.

2. MATERIALS AND METHODS

2.1. Data Collection

Publicly available metagenomic sequencing data were collected for 90 full-scale biogas reactors covering 58 cities in Eurasia (Data Set S1). The metagenomic data sets were generated from 10 individual studies, and the detailed accession information for sequences as well as the general operational conditions for these biogas reactors is listed in Data Set S1. Briefly, the operational temperature of biogas reactors ranged from 14 to 55 °C, and the reactors were categorized as ambient ($n = 17$), mesophilic ($n = 65$), and thermophilic digesters ($n = 8$). In addition, the substrates used for AD included agriculture wastes ($n = 12$), food wastes ($n = 3$), animal manure ($n = 75$), and wastewater sludges ($n = 15$). Considering animal feces contained a considerable amount of inherent ARGs as well as antibiotic residues, the biogas reactors were further divided into mature feed reactors ($n = 75$) and other reactors ($n = 15$) to facilitate statistical comparisons between group differences. A summary of the physiochemical and operational parameters of the biogas reactors is listed in Table 1.

Table 1. Summary of the Physiochemical and Operational Parameters of the Full-Scale Biogas Reactors Examined in This Study^a

	ambient	mesophilic	thermophilic
reactor number	17	65	8
temperature (°C)	16.8 ± 1.8	34.3 ± 5.8	52.4 ± 1.3
feed type	manure (17)	manure (51) others (14)	manure (7) others (1)
pH	8.2 ± 0.3	7.9 ± 0.5	8.1 ± 0.2
HRT (days)	55 ± 73	37 ± 44	15 ± 8
TAN (g-N/mL)	1.6 ± 1.5	2.5 ± 1.9	2.5 ± 0.6
VFA (g/mL)	0.5 ± 0.4	0.8 ± 1.3	0.7 ± 0.5
reference of data source	38	3,38–45	3,42,46

^aThe detailed information on the sample metadata of each reactor and data source is listed in Data Set S1. HRT: hydraulic retention time, TAN: total ammonia nitrogen, and VFA: volatile fatty acids.

2.2. Metagenomic Read-Based Analysis of Basic Resistome Traits

To guarantee the quality of the downstream analysis, quality filtration of raw metagenomic data was performed using Trimmomatic-0.39 with default parameters.⁴⁷ Kraken2 was applied to conduct taxonomic classification and quantify the corresponding relative abundance.⁴⁸ Microbial community composition (at phylum and genus levels) of all samples was provided in Figure S1 and Data Set S1. To profile the basic traits of the AD resistome including ARG diversity and abundance, ARG-like reads were predicted with ARGs-OAP3 using a similarity search against SARG v3.0 database,³⁶ with 80% of identity and 25 of alignment length cut-offs. ARG copy per cell (GPC) were used for the quantification of each ARG types.⁴⁹ The high-risk ARGs were identified with a previously proposed omics-based framework for assessing the health risk of ARGs (ARG-ranker framework),⁵⁰ as recently applied in risk assessment of soil ARGs.¹⁰

To reveal the co-occurrence patterns among ARG subtypes and microbial taxa, we constructed a correlation matrix by calculating all possible pairwise Spearman's rank correlation coefficients between the ARG subtypes and microbial genera.^{3,51} A correlation between two biological entities was considered significant if Spearman's correlation coefficient (ρ) was >0.8 and the FDR-adjusted P was <0.01 using the code "Co-occurrence_network.R" implemented in MbioAssy1.0 (<https://github.com/emblab-westlake/MbioAssy1.0>).^{3,52} Network analyses were performed in R environment using VEGAN,⁵³ igraph,⁵⁴ and Hmisc⁵⁵ packages. Network visualization was conducted on the interactive platform of Gephi.⁵⁶

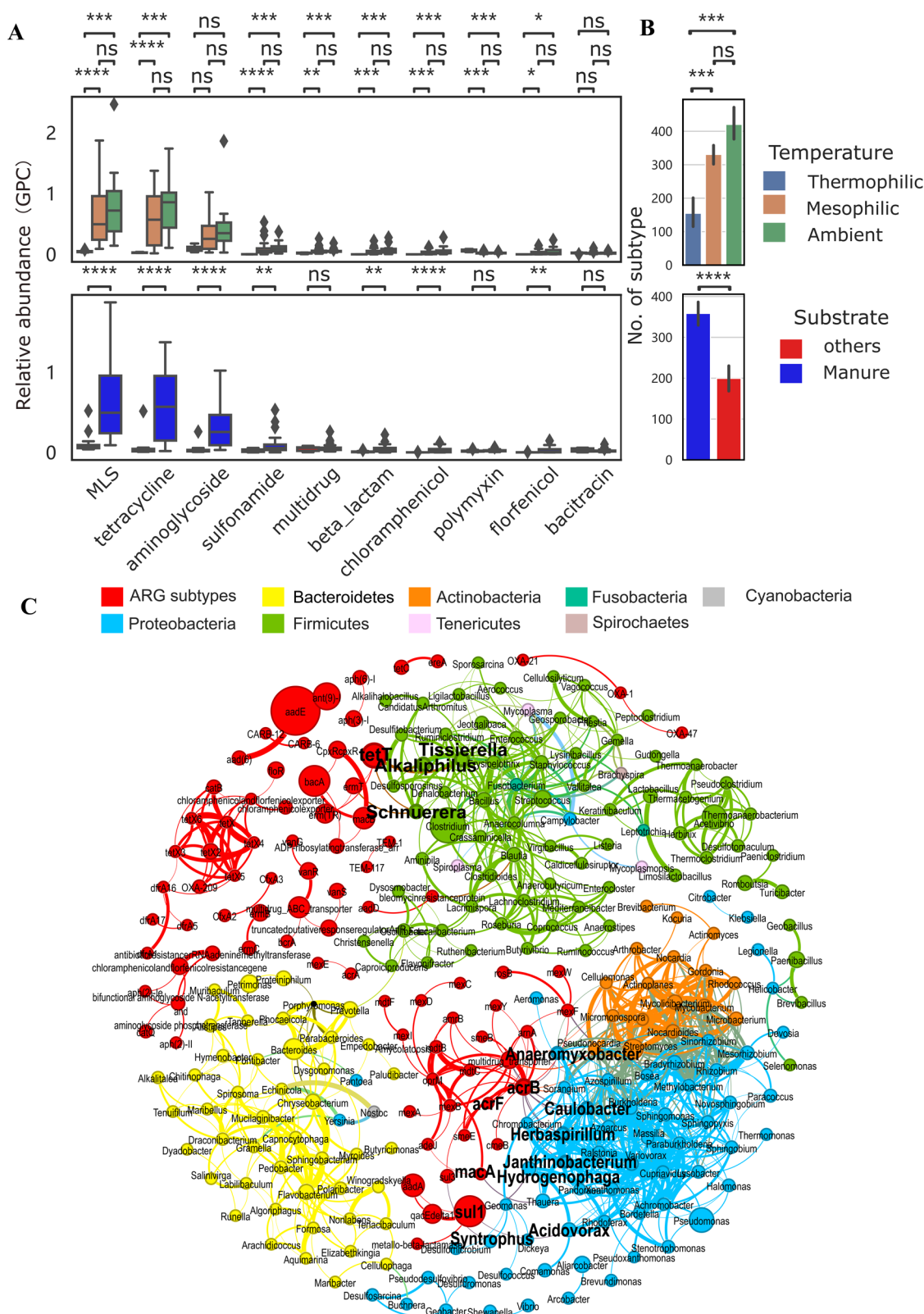


Figure 1. Overall ARG distribution in 90 full-scale biogas reactors. (A) Abundance (gene per cell, GPC) of ARG types in ambient (14–20 °C, $n = 17$), mesophilic (20–45 °C, $n = 65$), and thermophilic (45–54 °C, $n = 8$) reactors and the abundance (GPC) of ARG types in the manure fed ($n = 75$) and nonmanure fed biogas plants ($n = 15$). (B) Number of unique ARG subtypes identified in ambient, mesophilic, and thermophilic biogas plants. The statistical significance among different temperature and substrate groups was tested with the Mann–Whitney U test, ns: $P > 0.05$, *: $0.01 < P \leq 0.05$, **: $0.001 < P \leq 0.01$, ***: $0.0001 < P \leq 0.001$, ****: $P \leq 0.0001$. The specific p values are provided in [Data Set S4](#). (C) The co-occurrence networks between ARG subtypes and microbial taxa (genus). Each node represents an ARG (gene GPC) or a microbial genus (%) scaled by average relative abundance. Each connection or edge represents a strong (Spearman's correlation coefficient $\rho > 0.8$) and significant ($P < 0.01$) correlation within or between an ARG and a microbial genus. The nodes of the ARG-taxon associations were highlighted in bold.

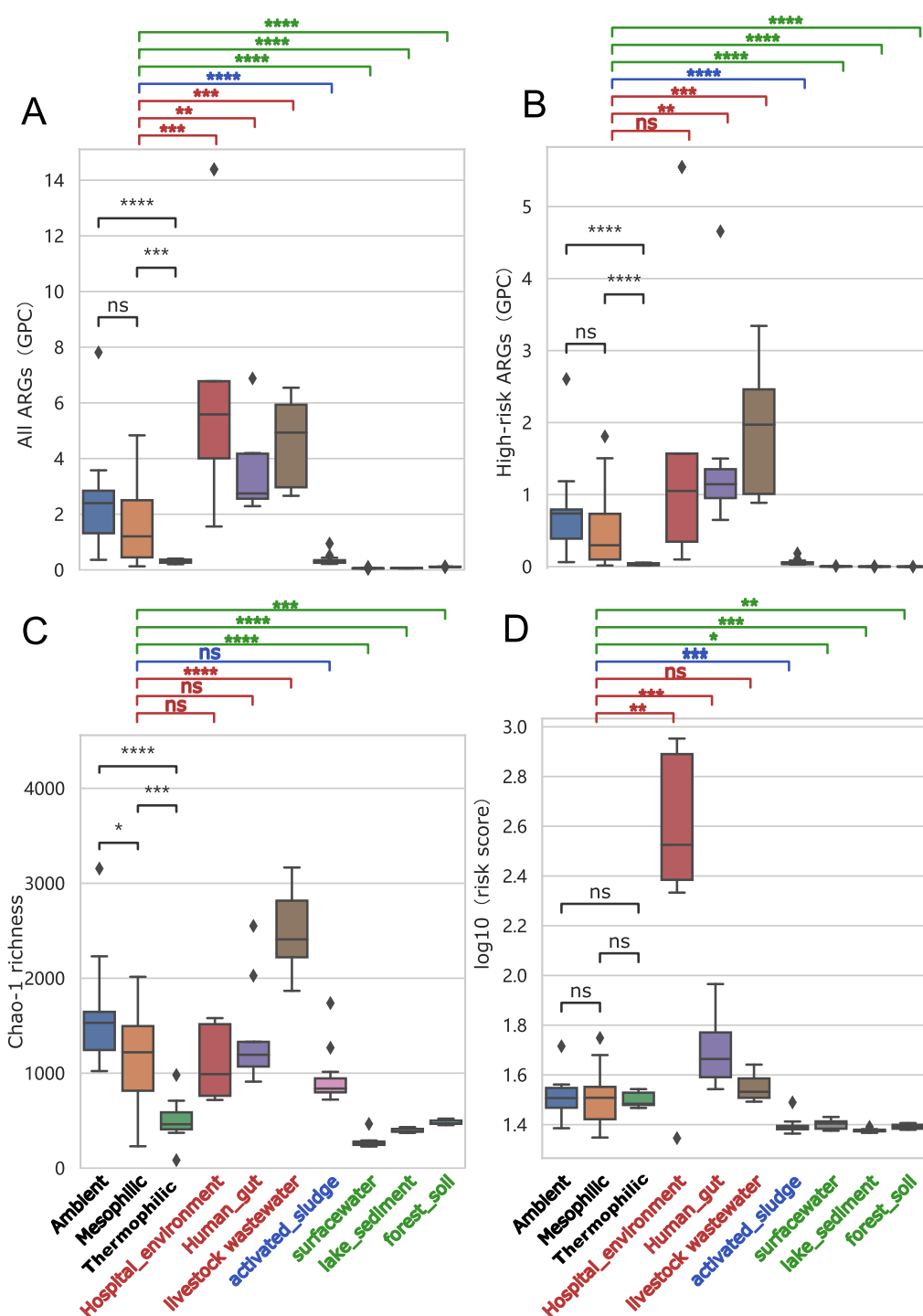


Figure 2. Comparison between AD resistome and other typical ecosystems. The boxplots showing comparison of total abundance of all ARGs (A), total abundance of high-risk ARGs (B) (i.e., Rank I and II ARGs determined in the ARG-ranker framework⁵⁰), chao1 richness of ARGs (C), and risk score (D) (calculated by the Metacompare⁶¹) between AD and other typical ecosystems including hospital environment ($n = 9$), human gut ($n = 9$), livestock waste, activated sludge ($n = 9$), surface water ($n = 9$), lake sediment ($n = 9$), and forest soil ($n = 9$). The color shadows were used to illustrate the microbiome types: the microbiome exposed to antibiotic selective pressure (red), the recently proposed ARG hotspot (blue), and natural environment (green).

2.3. Metagenomic Assembly-Based Analysis of Key Resistome Traits

2.3.1. Metagenome Assembly and Mobility Analysis. The quality-controlled sequences were assembled with metaSpades,⁵⁷ and the statistics of the metagenomic assemblies is provided in Data Set S2. The assembled plasmids were further classified into chromosome, plasmid, and viral contigs with geNomad using a marker set of

227,897 protein profiles specific to chromosomes, plasmids, or viruses.⁵⁸ The genome quality of Viral contigs was further evaluated using checkV,⁵⁹ and the results are listed in Data Set S3. The clean reads of the each samples were mapped to the corresponding metagenomes using bbmap⁶⁰ to calculate the coverage of the contigs as well as the genes on the contigs. The overall resistome risk score (evaluated based on the mobility and pathogenicity of ARGs) was calculated with the MetaCompare pipeline.⁶¹

2.3.2. Metagenome-Assembled Genome Construction, Taxonomy, and Phylogeny. To further investigate the taxonomy, phylogeny, and divergence of AD-ARGs, genome-centric metagenomic pipelines were used to recover metagenome-assembled genomes (MAGs). Briefly, the assembled contigs of each metagenomes were binned with metaBAT2.⁶² The draft genomes were dereplicated using dRep with a similarity of 98%. This similarity cutoff representing a subspecies level was chosen to recover the most diversity of ARG hosts.⁶³ The quality of each MAG was evaluated based on the completeness and contamination estimated with CheckM.⁶⁴ The taxonomy affiliation of each MAG was evaluated by GTDB-Tk (v0.3.2)⁶⁵ classify_wf. The average coverage of ORFs and MAGs was calculated based on reads recruitment by BBMap,⁶⁰ and the relative abundance of MAGs was calculated based on the average coverage in each sample. The data throughput during the metagenomic pipelines is presented in Figure S2.

2.3.3. Identification of Antibiotic Resistance and Virulence Factor Genes. The ORFs were predicted from contigs using Prodigal (v2.6.3). The ORFs were blast against SARG database using identity > 80 and coverage > 75 as criteria to identify the ARGs in the metagenomic-assembled contigs. The pathogenicity of MAG was evaluated with a previously developed strategy.³⁴ Briefly, the pathogenic MAGs were identified based on their taxonomy classification as well as the presence of virulence factor genes (VFGs). The VFGs were identified by BLASTN search against virulence factor database with identity > 70% as the cutoff.

2.3.4. Circular Genome Sequence Reconstruction and Functional Annotation. The MAG of *Escherichia coli* MAG6120 contained the most ARGs and was further used to reconstruct the complete, a circular chromosome sequence with MEDUSA using the genome sequence of its closest relative *E. coli* str. K-12 substr. MG1655 as a template.⁶⁶ The genes on the MAG6120 genome were predicted with Prodigal (v2.6.3) and functional annotated with eggNOG-mapper v2.⁶⁷ The genome of *E. coli* MAG6120 is visualized in the Artemis genome browser.

2.4. Statistical Analysis

All statistical analyses were considered significant at $p < 0.05$. Seaborn, statannot, and matplotlib libraries were used in Python to create the box plots and bar graphs. The comparison between antibiotic resistome of anaerobic digesters under many various operational conditions and other typical ecosystem samples was examined using the Mann–Whitney U test.

3. RESULTS

3.1. Diversity and Abundance of AD-ARGs in Global Biogas Digesters

To illustrate the basic resistome traits (i.e., ARG diversity and abundance) in AD systems, we first used ARGs-OAP3³⁶ to profile ARGs in all 90 full-scale biogas plant samples. The results show that the AD systems harbored 1.63 ± 1.43 GPC (i.e., gene GPC) of ARGs with an abundance peak (7.81 GPC) at an ambient manure-fed biogas plant (Figure 1 and Data Set S2). Among the 30 ARG types detected, macrolide–lincosamide–streptogramin (MLS), 0.55 ± 0.51 GPC), tetracycline (0.48 ± 0.44 GPC), aminoglycoside (0.29 ± 0.31 GPC), and sulfonamide (0.07 ± 0.09 GPC) are the four most abundant (Figure 1A), followed by multidrug, chloramphenicol and polymyxin. Moreover, the Mann–Whitney U test shows significant different patterns ($P < 0.05$) in both ARG abundance (Figures 1A and S3) and diversity (Figure 1B) between the AD systems grouped by the digestion temperature (ambient, mesophilic vs thermophilic) and feedstock substrate (manure vs nonmanure). On one hand, higher temperature biogas plants have significantly lower ($P < 0.05$) abundance in 11 ARG types, including tetracycline, MLS, sulfonamide, and so on (Figure 1A). On the other hand,

manure-fed biogas plants (as the solo or a codigestion substrate) show a significantly higher ($P < 0.05$) abundance in 12 ARG types, especially for tetracycline, MLS, and aminoglycoside (Figure 1A). Diversity wise, thermophilic condition AD microbiome carries on average 155 ± 66 ARG subtypes, which is significantly lower than ambient (421 ± 105) and mesophilic conditions (331 ± 114). Similarly, the manure fed reactors (359 ± 119) show significantly higher ARG subtypes compared with other biogas plants (200 ± 64) (Figure 1B). These results suggest the digestion temperature and feedstock substrate as two major operational parameters influencing a resistome structure in global biogas plants.

The co-occurrence patterns between ARG subtypes and microbial taxa (genus level) in the AD systems were interactively explored with network analysis (Figure 1C). The topological properties are summarized in Text S1. The results of network analysis show significant and strong co-occurrence associations (Spearman's rank coefficient $\rho > 0.8$, FDR-adjusted $P < 0.01$) among 84 ARG subtypes and 204 bacteria genera. On one hand, the large number of ARG–ARG associations (118 instances) and the taxon–taxon associations (894 instances) could reflect or be derived from (i) coselection or genome collinearity of ARGs³ and (ii) microbial niche overlap or biotic interactions,⁵² respectively. On the other hand, a few significant ARG–taxon associations (22 instances) implied potential community-wide host–ARG relationships.⁵¹ For example, *Schnuerera*, *Tissierella*, and *Alkaliphilus* are the potential bacterial hosts of tetracycline-resistant gene *tetT* in the global anaerobic digesters. The notable lack of significant pairwise correlations between most ARG subtypes (11.48%) and microbial taxa implies the high complexity and multidimensionality of relationships among ARG subtypes and their broad range of bacterial hosts, e.g., a microbial taxon could be the host of multiple ARGs or an ARG subtype can be hosted by multiple taxa.

3.2. Comparing AD Resistome with Other Ecosystem Habitats

To rationally evaluate the selection level of antibiotic resistance in the global AD systems, we further compared the abundance and diversity of AD-ARGs with three groups of typical reservoirs of ARGs, including (i) those under heavy antibiotic selective pressure (hospital environments, human gut, and livestock wastewater), (ii) the recently proposed hotspots of ARG (activated sludge),¹⁴ and (iii) representative natural habitats (surface water, lake sediment, and forest soil) (Figure 2A–C). Considering the overall ARG abundance, the AD systems show a significantly higher ARG abundance than the natural habitats but a lower ARG abundance than those reservoirs under presumably heavier antibiotic selective pressure. Specifically, ambient and mesophilic AD systems show 3.5–5.9 times higher ARG abundance (1.59 – 2.44 GPC) compared with activated sludge (0.35 ± 0.18 GPC), while thermophilic AD systems have highly similar ARG abundance (0.31 ± 0.07 GPC) with activated sludge, revealing that the digestion temperature positively relates with a low ARG abundance. Focusing on the high-risk ARGs (i.e., mobilizable, pathogen-carriable, and clinically relevant ARGs¹⁰), it should be noted that the ambient and mesophilic AD systems even show a similar abundance with hospital environments.

Further, the diversity of AD-ARGs was estimated with Chao1 richness and compared with the resistome diversity of other ecosystem habitats. The results indicate that ambient and

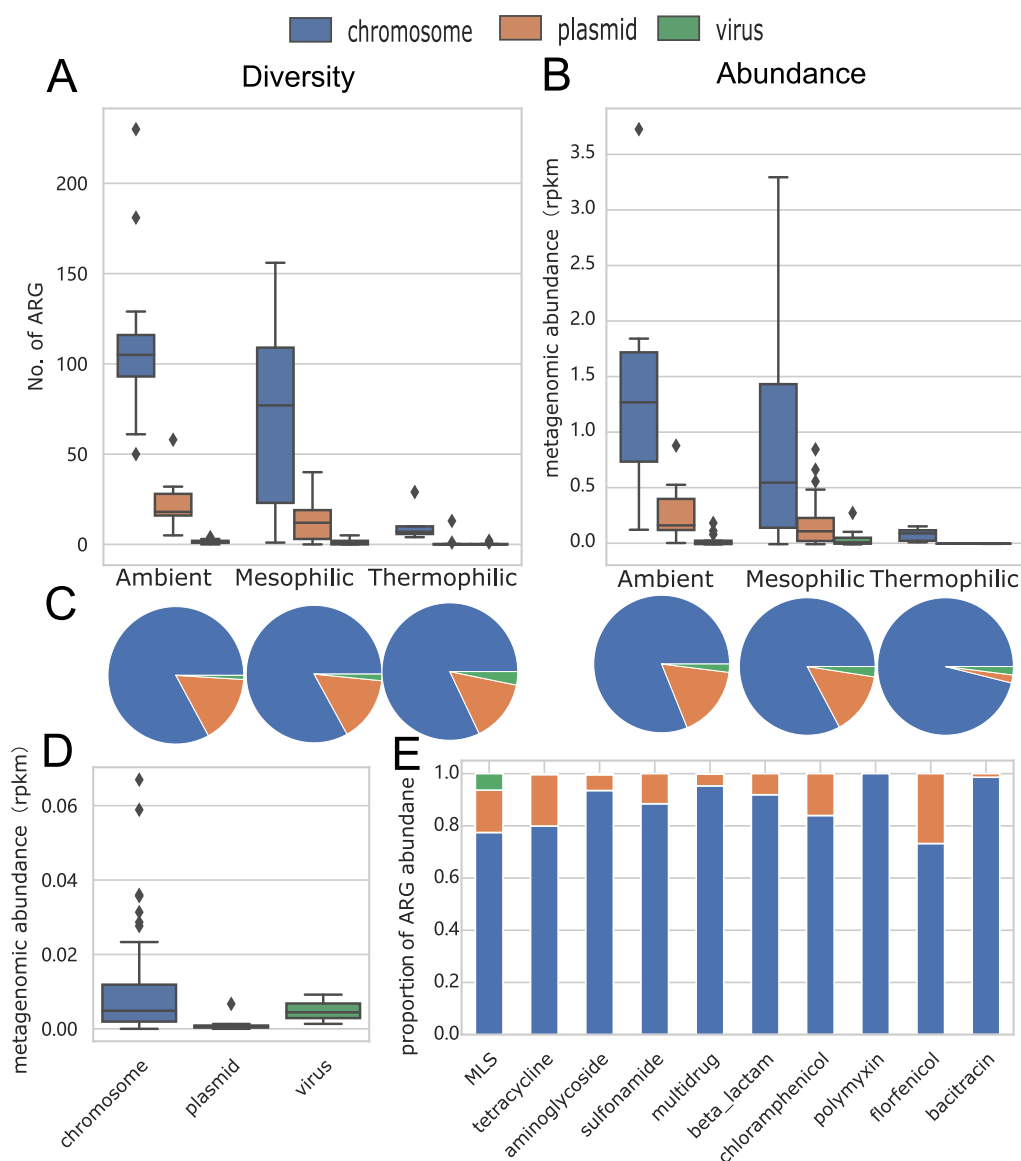


Figure 3. Mobility of AD-ARGs. (A) Number of ARGs located on chromosomes, plasmids, and viruses contigs. (B) Relative abundance (rpkm) of ARGs located on chromosomes, plasmids, and virus contigs. (C) Proportion of ARGs on chromosomes, plasmids, and viruses based on the number of ARGs (the left three pies) and abundance (the right three pies) under ambient, mesophilic, and thermophilic conditions. (D) Relative abundance (rpkm) of chromosomes, plasmids, and viruses encoding ARGs under thermophilic conditions. (E) Distribution of chromosomes, plasmids, and viruses encoding ARGs (based on average rpkm) in different types.

mesophilic AD resistomes show similar or higher ARG diversity than hospital environments and human gut resistome, while the thermophilic AD resistome show a similar ARG diversity with the natural environmental (i.e., surface water, lake sediment, and forest soil) resistomes (Figure 2C). Moreover, compared with thermophilic AD systems, both the ambient and mesophilic AD systems harbor a much higher number and fraction of ARG subtypes that could coexist in clinically relevant habitats (Figure S4). This result suggests that the land application of AD digestate could potentially increase the environmental antibiotic resistance level, posing an additional health risk. Combined, the results conclude on a significant role of temperature elevation in reducing the overall diversity and abundance of ARGs including high-risk ones in global biogas digesters.

The relatively high AMR risks of the AD system are also evidenced by the integrated risk score calculated by

Metacompare software considering the mobility and pathogenicity (Figure 2D). As the evaluation of the mobility and pathogenicity incidence of ARGs required resistome profiling on contig and MAG level (presented in the following sections), the detailed results on the Metacompare risk assessment are presented in the Discussion section.

3.3. Mobility Level of AD-ARGs in Global Biogas Digesters

Environmental microbiomes can harbor plasmid- and virus-mediated ARGs of anthropogenic origins. These mobile ARGs can be horizontally transferred among microbes through plasmid conjugation and viral transduction. To evaluate the mobility level of AD-ARGs, the 90 metagenomes of AD systems were de novo assembled using metaSpades algorithm, resulting in over 10 million contigs with an average N50 of 13 kb. The contigs were further classified as the chromosome, plasmid, and virus contigs using geNomad.⁵⁸ As a result, 96%

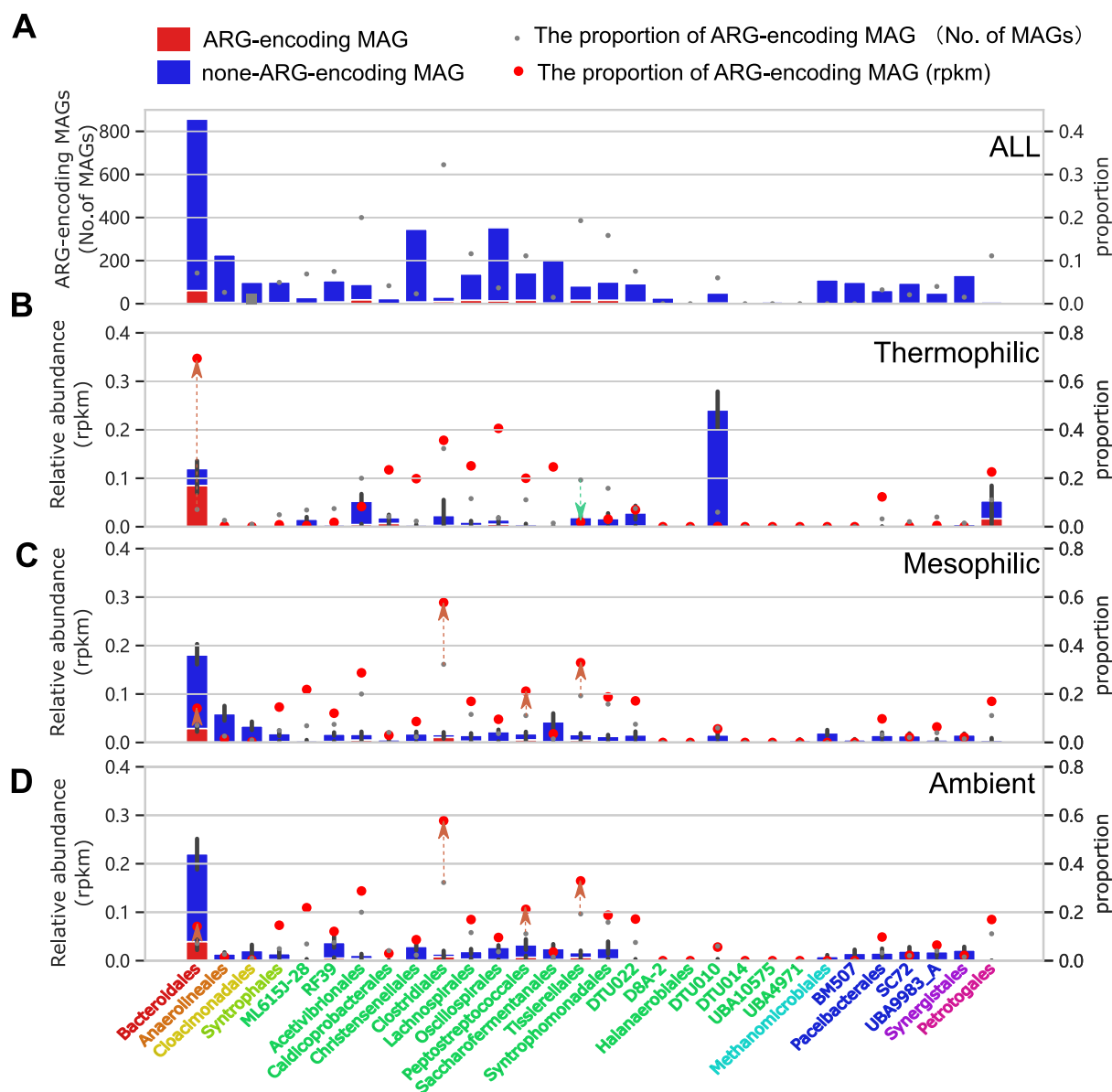


Figure 4. Comparison between the ARG encoding and non-ARG encoding MAGs from the abundant (top 5%) orders in AD microbiome. (A) Number of ARG-encoding MAGs and non-ARG-encoding MAGs in the abundant orders. (B) Relative abundance (rpkm) of ARG-encoding MAGs and non-ARG-encoding MAGs in the abundant orders under thermophilic conditions. (C) Relative abundance (rpkm) of ARG-encoding MAGs and non-ARG-encoding MAGs in the abundant orders under mesophilic conditions. (D) Relative abundance (rpkm) of ARG-encoding MAGs and non-ARG-encoding MAGs in the abundant orders under ambient conditions.

of the AD metagenome contigs are classified as chromosomes, 3% as plasmids, and 1% as viruses.

Further, protein-coding gene prediction from the above-mentioned metagenome-assembled contigs resulted in a total of 45,774,877 ORFs, of which 7779 are classified as ARGs distributed onto 6839 contigs. The identified ARG-ORFs belong to 21 types, corresponding to the abundant ARG types detected with short read prediction (average GPC > 0.00006). Among all the ARG-ORFs, more than 80% are located or encoded on the chromosomes, ~16% on the plasmids, and less than 2% on the viruses. The diversity distribution among chromosomes, plasmids, and virus-encoded ARGs shows similar profiles in ambient, mesophilic, and thermophilic AD systems (Figure 3A). Considering the relative abundance (rpkm) of ARGs in each metagenome, a similar distribution among chromosomes, plasmid, and virus ARGs is found in

ambient and mesophilic AD systems (Figure 3B). Notably, plasmid ARG accounted for only 2% in abundance of overall ARGs in the thermophilic digesters, which is significantly lower than the portion (14%, $P < 0.05$) of plasmid ARGs among all ARGs in the thermophilic digesters (Figure 3C). Specifically, the plasmid ARGs show a significantly lower abundance in the thermophilic AD microbiome than the chromosomal ARGs (Figure 3D).

In addition, the distribution of ARG locations (chromosomes, plasmids, or viruses) shows notable differences among ARG types (Figure 3E). In brief, a relatively large portion of plasmid ARGs are assigned to florfenicol (27%), tetracycline (20%), and MLS (16%). This result suggests a high possibility for florfenicol, tetracycline, and MLS to horizontally spread between bacteria within the AD microbiome through conjugation. On the contrary, most aminoglycoside ARGs

Table 2. Genome Quality, Taxonomy, Detection Frequency, and Resistance Profile of Pathogenic AD-MAGs^a

MAG ID	genome quality		taxonomy and pathogenicity		detection		resistance profile		
	completeness %	contamination %	genus assigned	no. of VF	mesophilic	ambient	no. ARG	type	subtype
MAG5509	94.27	2.28	<i>Bacteroides</i>	1	12:65	7:17	0	n.d	n.d
MAG2206	93.25	0.95	<i>Corynebacterium</i>	5	2:65	2:17	1	multidrug	mtrA
MAG759	94.54	0.33	<i>Enterococcus</i>	1	28:65	8:17	2	chloramphenicol	acetyltransferase
MAG5418	84.57	1.32	<i>Enterococcus</i>	2	4:65	1:17	0	n.d	n.d
MAG6120	97.88	0.35	<i>Escherichia</i>	76	1:65	2:17	70 ^b	multidrug, polymyxin and etc.	emrY, eptA, and etc.
MAG5455	98.91	0	<i>Morganella</i>	7	0:65	1:17	7	bacitracin, multidrug, beta_lactam	bacA, mdtG, rsmA, CRP, _DHA-20, emrB
MAG4933	95.47	1.57	<i>Pseudomonas</i>	2	5:65	1:17	1	multidrug	rsmA
MAG1488	95.28	0.5	<i>Pseudomonas</i>	1	9:65	1:17	1	multidrug, polymyxin	rsmA
MAG256	95.24	1.15	<i>Pseudomonas</i>	3	6:65	0:17	1	multidrug	rsmA
MAG1230	94.9	0.93	<i>Pseudomonas</i>	2	7:65	0:17	5	multidrug, bacitracin, trimethoprim	rsmA, MuxB, bacA, rsmA_dfrA1
MAG4998	93.93	0	<i>Pseudomonas</i>	44	5:65	4:17	2	multidrug	MexD, rsmA
MAG500	87.84	1.45	<i>Pseudomonas</i>	60	1:65	2:17	2	multidrug	MexB, rsmA
MAG3630	85.91	5.07	<i>Pseudomonas</i>	5	11:65	2:17	2	multidrug, bacitracin	bacA, rsmA
MAG495	84.17	0.43	<i>Pseudomonas</i>	4	4:65	1:17	1	multidrug	rsmA
MAG2742	82.05	1.44	<i>Pseudomonas</i>	2	14:65	2:17	1	multidrug	rsmA
MAG5897	81.03	0	<i>Pseudomonas</i>	75	3:65	1:17	4	multidrug	MuxB, YajC, bacA, rsmA
MAG4959	71.71	1.72	<i>Pseudomonas</i>	1	4:65	0:17	1	multidrug	rsmA
MAG4843	63.16	1.75	<i>Pseudomonas</i>	40	2:65	1:17	5	multidrug, bacitracin	mexK, bacA, mexW, MexF, mexK
MAG 4819	61.4	0	<i>Pseudomonas</i>	75	2:65	0:17	5	multidrug, bacitracin	mexK, CpxR, mexW, bacA, YajC

^aAD: anaerobic digestion; MAG: metagenome-assembled genome. The full resistance profile of MAG6120 was visualized in Figure 5 and Data Set S6. ^bThe number reflects the ARGs annotated with both SARG and CARD databases using blast and RGI.

(>93%) were located on chromosomes, implying that they are unlikely to horizontally spread among AD bacteria. In addition to the ARG locations, the similarity between ARG-ORFs is calculated to find the identical ARGs that are placed on multiple contigs in individual biogas reactors (Data Set S8). As a result, a total of 56 pairs of ARGs are identified in 30 samples. Those ARGs only account for a tiny fraction of the overall resistome (less than 2% on abundance and less than 0.1% on diversity), implying a limited number of recent horizontal ARG transfer events in the investigated AD microbiome.

3.4. Host Identity of AD-ARGs in Global Biogas Digesters

To explore the host identity and pathogenicity of AD-ARGs, a nonredundant set of metagenome-assembled genomes (MAGs) consisting of 6750 members at a subspecies level (98% similarity) was constructed and labeled “AD-MAG”. Based solely on the completeness and contamination of AD-MAGs,⁶⁸ the data sets compose of 20.5% high-quality (completeness > 90%, contamination > 90%), 40.8% medium-quality (completeness > 50%, contamination < 10%), and 36.7% low-quality members (completeness < 50%, contamination < 10%). Considering the number of reads mapped, the AD-MAG set accounts for a total of 69% metagenomic reads and thus represents the major microbiome members in the AD system with various operational temperatures and substrate types (Figure S2). The list of all MAGs and their quality are provided in Data Set S5.

Within the set of 6750 AD-MAGs constructed from 90 full-scale biogas reactors, 762 ARGs are identified, among which 182 ARGs are prevalent and presented (average coverage > 1)

in more 50% of AD samples ($n = 45$). Specifically, more than 6% ($n = 467$) carry at least 1 copy of ARGs, accounting for 0.11 copies of ARG per genome on average. The hosts of AD-ARG cover all major taxa in the AD microbiome, including 34 prokaryotic phyla broadly distributed into 54 classes and 96 orders. The number of ARG-encoding MAGs and all MAGs in each bacterial order is listed in Data Sets S1–S8, and the results of the representative taxa are presented in Figure 4A. The results indicate that among all the abundant orders encode ARGs, including the *Clostridiales* (31 MAG, 32% carrying ARGs), *Acetivibrionales* (90 MAG, 20% carrying ARGs), and *Tisslerellales* (83 MAG, 19% carrying ARGs). The above-mentioned bacterial orders were well-known fermenting members in AD consortia. Different from the above-mentioned fermenters, the typical syntrophic acid oxidizing members, such as *Syntrophales* ($n = 101$) and *Synergistales* ($n = 132$), show generally lower richness of ARGs, with only 5% and 2% MAGs-encoding ARGs, respectively. The order *Bacteroidales* shows the highest species diversity among all orders with 857 MAG representatives, 7% of which carried at least one copy of ARG ($n = 61$). The *Bacteroidales* members constitute the largest portion of the ARG-encoding MAGs (13%).

Although only 6% of MAGs in the AD-MAG set carried identifiable ARGs, they contribute to 15%, 10%, and 12% of MAG relative abundance in thermophilic, mesophilic, and ambient AD digesters, respectively. Figure 4B,C presents the relative abundance most important AD orders and the proportion between ARG-encoding and non-ARG-encoding MAGs. The results show that the ARG-encoding *Bacteroidales* members account for 71%, 16%, and 18% in thermophilic,

INFORMATION STORAGE AND PROCESSING METABOLISM

Translation, ribosomal structure and biogenesis
RNA processing and modification.
Transcription
Replication, recombination and repair

POORLY CHARACTERIZED

Function unknown
not predicted

Energy production and conversion
Carbohydrate transport and metabolism
Amino acid transport and metabolism
Nucleotide transport and metabolism
Coenzyme transport and metabolism
Lipid transport and metabolism
Inorganic ion transport and metabolism
Secondary metabolites biosynthesis, transport and catabolism

CELLULAR PROCESSES AND SIGNALING

Cell cycle control, cell division, chromosome partitioning
Defense mechanisms
Signal transduction mechanisms
Cell wall/membrane/envelope biogenesis
Cell motility
Intracellular trafficking, secretion, and vesicular transport
Posttranslational modification, protein turnover, chaperones

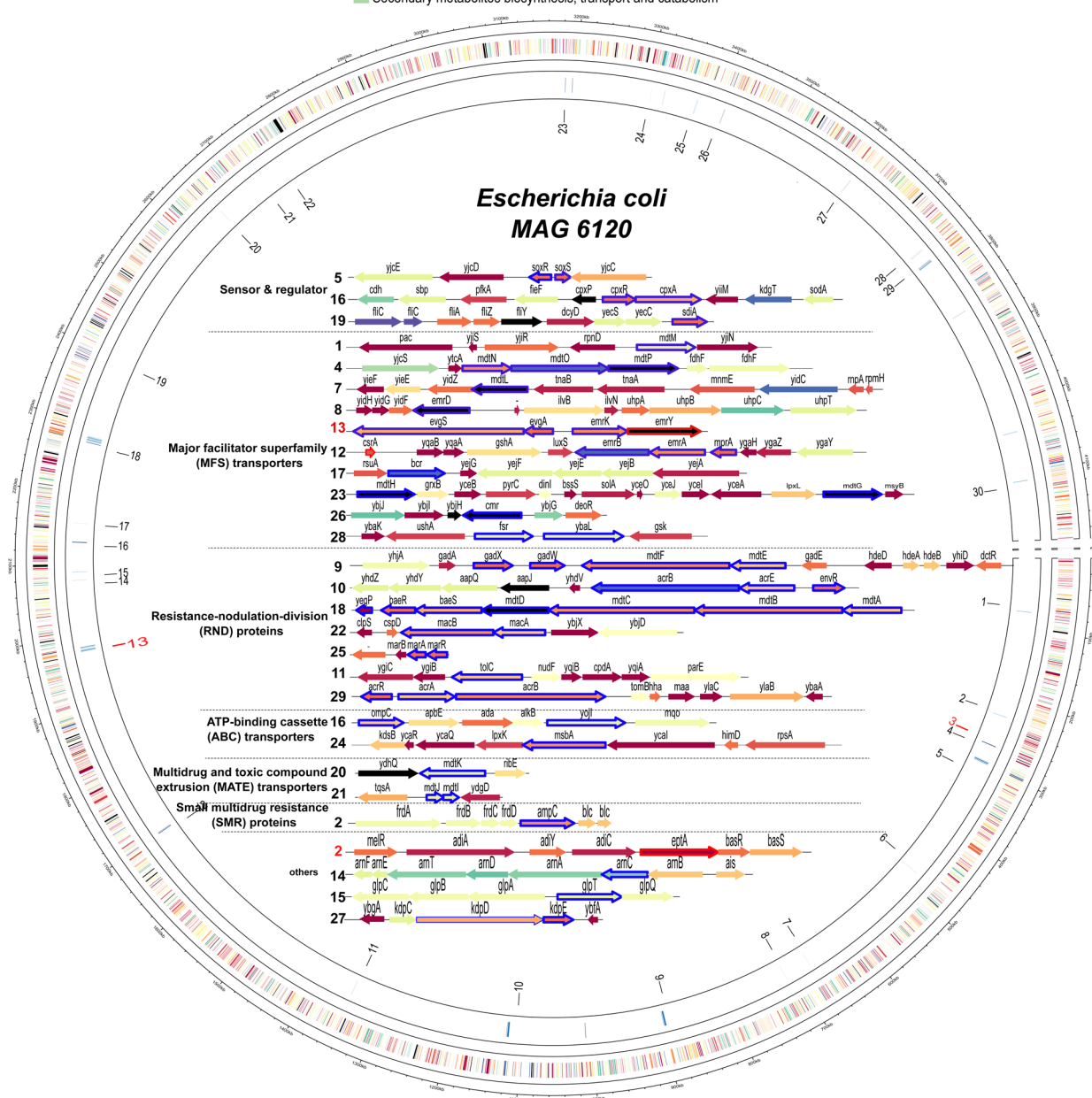


Figure 5. Reconstruction of *E. coli* MAG6120 and the distribution of ARGs on the genome. The numbers before each ARG operon indicated its position on the genomes. The color of genes was its function categorized by the clusters of orthologous groups. The red notation represents the two high risk ARGs carried by *E. coli* MAG6120.

mesophilic, and ambient AD microbiomes, respectively, which is 2–3 times higher than the number of ARG encoding MAGs among all MAGs in the same order (7%). The observation suggests that the ARG-encoding *Bacteroidales* members show a higher fitness in AD systems compared to the non-ARG encoding members, especially under higher operational temperatures. Additionally, the manure-fed biogas reactors show a significantly higher abundance of ARG-encoding *Bacteroidales* MAGs (Figure S5) than other biogas reactors, suggesting those MAGs potentially come with the manure feedstock and retain their relative abundance in the AD

systems. Nevertheless, this hypothesis needs to be confirmed in future studies that perform large-scale sequencing investigations of AD feedstocks. Similarly, the relative abundance of ARG-encoding *Clostridiales*, *Tissierellales*, and *Peptostreptococales* MAGs also shows a disproportionately high relative abundance compared with the number of ARG-encoding MAGs among all MAGs in this order under ambient and mesophilic conditions.

3.5. Host Pathogenicity and Multiresistance Properties

The pathogenicity of the MAGs was evaluated based on the taxonomy information evaluated by gtdbtk (v0.3.2)⁶⁵ and the presence of VFG in each genome. As a result, 21 pathogenic MAGs are identified from the AD-MAG set, including members from *Pseudomonas* (15), *Enterococcus* (2), *Bacteroides* (1), *Corynebacterium* (1), *Escherichia* (1), and *Morganella* (1). The pathogenetic MAGs are only detected in mesophilic and ambient AD digesters. Among the 21 pathogenic MAGs, 19 MAGs encode at least 1 copy of ARGs. The detailed information on AD-pathogenic MAGs is presented in Table 2. The results show that the most detected pathogen MAGs in AD systems is an *Enterococcus* member encoding two copies of chloramphenicol acetyltransferase, with 43% and 47% detection rates in mesophilic and ambient reactors.

Among all the pathogenetic MAGs, an *E. coli* MAG carries the largest number of ARGs, i.e., 50 ARGs from 6 types, namely, Multidrug (40), Polymyxin (4), MLS (3), Beta_lactam (1), Bacitracin (1), and Other_peptide_antibiotics (1) according to SARG databases (V3.2). To further reveal the location of the ARGs on the *E. coli* genome, the genome of *E. coli* MAG6120 was chiralized using *E. coli* str. K-12 as a reference. Moreover, the genes from *E. coli* MAG6120 were further compared to CARD databases³⁵ to find additional ARGs. As a result, an additional 20 ARGs are identified. Most of the ARGs uniquely identified by CARD databases are subunits of antibiotic efflux pump proteins. The genome reconstruction showed that the ARGs scattered on the *E. coli* MAG6120 (Figure 5) and detailed ARGs lists are presented in Data Set S6. The result showed that *E. coli* MAG6120 has shown genetic potential for many types of effluent pump systems including the major facilitator superfamily transporters ($n = 10$), resistance-nodulation-division proteins ($n = 7$), ATP-binding cassette transporters ($n = 2$), multidrug and toxic compound extrusion transporters ($n = 2$), and small multidrug resistance proteins ($n = 1$). Moreover, the MAG is also equipped with multiple sensors and regulator proteins to activate the effluent pumps. Among all the ARGs carried by MAG6120, *eptA* and *ermY* are classified as “current threat” ARGs.⁵⁰ The former *eptA* was originally identified in *Salmonella enterica*, mediating phosphoethanolamine modification of lipid A and conferring resistance to polymyxin.⁶⁹ According to the prevalence data in CARD databases, *eptA* has been identified in the chromosome and plasmids of many pathogens, including *E. coli*. The latter *ermY*, together with it upstream *ermK*, has been previously proved to be active in *E. coli* under subinhibitory concentration of tetracycline, chloramphenicol, or salicylate, acting as a multidrug efflux pump. In summary, the results suggest *E. coli* MAG6120 as a multidrug-resistant pathogen that can pose substantial risks to human health.

4. DISCUSSION

With the growing realization of the One Health concept that integrates human, animal, and environmental health, the various habitats, including the AD systems examined in this study, are considered as important environmental reservoirs of ARGs. In this study, we characterized the AD resistome of 90 full-scale biogas digester facilities and illustrated both basic traits (i.e., abundance and diversity) and key traits (i.e., mobility, host identity, pathogenicity, and multiresistance) of AD-ARGs shaping the overall resistome risks. The results show

that AD systems present a relatively high resistome risk profile in terms of high diversity and high abundance for both all- and high-risk ARGs, compared with natural habitats such as soil, lake sediment, and surface water. Herein, we further assessed the resistome risk of AD systems based on quantitative basic traits and the qualitative key traits and highlighted an important role of evaluated digestion temperature in ARG reduction and risk mitigation.

4.1. AD Resistome Poses Critical Risks to the Environment

Based on metagenomic read-based analysis of basic traits of AD-ARGs, we find that compared with the natural habitats and engineered systems like activated sludge (Figure 2), mesophilic and ambient AD systems harbor a significantly higher abundance of both the total ARGs and high-risk ARGs (which were priorly ranked as mobilizable, pathogen-carriable, and clinically relevant by a ARG-ranker framework⁵⁰), suggesting a potential health risk in the release of their resistance loads to the environments. The relative abundance profiles of ARGs based on contig-level and MAG-level metagenomic analyses also align with read-level analysis and support the aforementioned discussion on the relative abundance of ARGs. Besides the abundance, the AD system also showed significantly higher ARG diversity than natural environments (Figure 2).

In addition to the basic quantitative resistome traits discussed above, the key qualitative traits such as the mobility and host pathogenicity of ARGs are also considered. Within the set of AD-MAGs, 16% ARGs are located on plasmid contigs, implying their potential mobility, accounting for 16% and 15% ARG abundance in ambient and mesophilic digestors. It is known that the ARG encoding plasmid typically poses a biosynthesis burden to the bacterial host, and such plasmids were easily lost without selective pressure.⁷⁰ The presence of considerable ARG encoding plasmids implies a potential antibiotic resistance pressure, possibly from the antibiotic residues from farming or other anthropogenic activity. In addition to the plasmid conjunction, viral transduction could be another potential pathway for ARG spread in the AD microbiome. In the current study, we identified 96 putative viral contigs encoding ARGs mainly from unclassified *Caudoviricetes* (Data Set S3). However, the viral contigs identified in the current study are highly fragmented possibly due to the lower coverage or insufficient sequencing depth to effectively recover the viral genomes in AD microbiomes. Future studies dedicated to unveiling the AD viral diversity are encouraged to further reveal how much viral transduction may promote the spread of AD-ARGs. Although the current study mainly evaluated the mobility of ARGs by its location on a plasmid or viral contigs, it needs to be clarified that chromosomal ARGs also have mobile potentials through the presence of mobile genetic elements (MGEs). In this study, we failed to identify any high confidence (>80% identity and >70% alignment percentage) MGEs by comparing all ORFs on ARG-encoding contigs to the mobileOG database.⁷¹ However, it is still possible that the chromosomal ARGs are mobile through unidentified MGEs that do not meet the aforementioned high-confidence alignment cutoffs.

Besides mobility, host pathogenicity of ARGs is another risk-associated aspect of resistome key traits. Most pathogenic MAGs identified in AD systems (19/21) carry at least one copy of ARGs, most of which are functionally assigned to a multidrug effluent pump. The prevalence of ARGs in

pathogenic bacteria alerts a potential health risk of an AD effluent.

To comparatively evaluate the overall resistome risks, we calculated the Metacompare risk score of the global AD resistome (considering the mobility and pathogenicity incidence). The result indicates that its average risk score (32.0) is comparable with high-risk livestock wastewater (35.7, $P > 0.05$), while being significantly higher than the activated sludge (24.8, $P < 0.05$), forest soil (24.7, $P < 0.05$), lake sediment (23.8, $P < 0.05$), and surface water (25.2, $P < 0.05$) (Figure 2). These results suggest that the AD systems are important ARG reservoirs and the resistome mitigation is encouraged before the land application of AD digestate.

4.2. Thermophilic Operation Mitigates AD-ARGs and Resistome Risks

Comparing the quantitative basic traits and qualitative key traits of resistome in AD systems under different temperatures, the results reveal that on a global scale thermophilic digesters show 78% and 85% less abundant ARGs than mesophilic and ambient digesters, especially from several types, including tetracycline, MLS, and Phenicol. In addition to the relative abundance, the thermophilic AD resistome also comprises 68% and 62% less ARG subtypes than mesophilic and ambient digesters, showing a significantly lower resistome diversity. The finding consists of the priorly reported ARG reduction improvements during the temperature transition from mesophilic to thermophilic conditions,⁷² suggesting that a high operational temperature could effectively reduce AD-ARGs and mitigate the resistome risk. In addition to the overall lower ARG abundance and diversity, the high temperature also decreased the presence and abundance of super ARG hosts and pathogens, leading to an overall reduced health risk. Our results show that all pathogenic MAGs are not detected in thermophilic AD digesters.

It is widely accepted that thermophilic AD systems could efficiently mitigate the growth of pathogens because the operational temperatures can effectively inactivate and eliminate many pathogens.⁷³ It is widely accepted that thermophilic AD systems could efficiently mitigate the growth of pathogens because the operational temperatures can effectively inactivate and eliminate many pathogens. In addition to pathogen control, the thermophilic operation conditions mitigate AMR risks through an intricate mechanism. A high operational temperature leads to a faster organic conversion rate and consequently results in shorter HRTs and higher organic loading rates than for the operation of mesophilic and ambient reactors. Specifically, the average HRT of thermophilic reactors in the current data set is 15 days, which is significantly lower than the mesophilic (37 days) and ambient (55 days) reactors examined in this study (Table 1 and Data Set S1). The shorter HRTs limited the exposure time of AD functional microbes to the potential toxicants in AD sludges (i.e., antibiotics, disinfectants, and heavy metals), therefore posing a low selective pressure for the thermophilic AD microbes to carry ARGs or disseminate them. In addition, the thermophilic condition was also suggested to remove ARGs by reducing the microbial diversity, considering the prior study showing that potential ARG hosts from *Proteobacteria*, *Bacteroidetes*, and *Actinobacteria* were suggested to hardly survive under thermophilic conditions.²¹ In the current study, the mobility analysis of ARGs showed a significantly lower abundance of plasmid ARGs under

thermophilic conditions. One explanation of the ARG mitigation under thermophilic conditions is that the high temperature increases the metabolic burden on bacterial cells, particularly when expressing recombinant proteins for plasmid amplification in the hosts.⁷⁴ This added stress can also negatively affect plasmid stability and spread and therefore hinder the mobility of ARGs.⁷⁰ Although previous studies argued against the rationale behind the further increase of the temperature to thermophilic condition (55 °C) in specific cases,^{20,21} the current results clearly demonstrated the overall benefits of relatively higher temperature AD from an underappreciated perspective of resistome risk mitigation.

■ ASSOCIATED CONTENT

Supporting Information

The Supporting Information is available free of charge at <https://pubs.acs.org/doi/10.1021/acsenvironau.4c00071>.

Microbial community composition (at phylum level) of 90 samples revealed by Kraken; data throughput during the metagenomic pipelines; overall ARG distribution in 90 full-scale biogas reactors; Venn diagram of the ARG subtypes in AD systems, nature habitat; relative abundance of ARG-encoding and non-ARG-encoding *Bacteroidales* MAGs in different feedstock biogas reactors; and comparison of the ARG abundance revealed by read-, contig, and MAG-level metagenomic analyses (PDF)

Sample metadata of the 90 full scale biogas plants used in the current study; assemble statistics of the 90 metagenomic samples; genome quality of all viral contigs; significance between the relative abundance (GPC) of ARGs in each type; list of all MAGs and their quality; ARGs carried by *E. coli*MAG5498; contig level ARG identification; and identical ARG pairs in the individual biogas reactor samples (XLS)

■ AUTHOR INFORMATION

Corresponding Author

Feng Ju – Westlake Laboratory of Life Sciences and Biomedicine, School of Life Sciences, Westlake University, Hangzhou 310024, China; Environmental Microbiome and Biotechnology Laboratory, School of Engineering and Center of Synthetic Biology and Integrated Bioengineering, Westlake University, Hangzhou 310030 Zhejiang, China; Institute of Advanced Technology, Westlake Institute for Advanced Study, Hangzhou 310024 Zhejiang, China; orcid.org/0000-0003-4137-5928; Phone: 571-87963205; Email: jufeng@westlake.edu.cn; Fax: 0571-85271986; www.ju-emblab.com

Authors

Xinyu Zhu – Westlake Laboratory of Life Sciences and Biomedicine, School of Life Sciences, Westlake University, Hangzhou 310024, China; Environmental Microbiome and Biotechnology Laboratory, School of Engineering and Center of Synthetic Biology and Integrated Bioengineering, Westlake University, Hangzhou 310030 Zhejiang, China

Irini Angelidaki – Department of Chemical and Biochemical Engineering, Technical University of Denmark, Kgs. Lyngby DK-2800, Denmark

Tong Zhang – Environmental Microbiome Engineering and Biotechnology Laboratory, Department of Civil Engineering,

The University of Hong Kong, Pokfulam 999077, Hong Kong, China; orcid.org/0000-0003-1148-4322

Complete contact information is available at:

<https://pubs.acs.org/10.1021/acsenvironau.4c00071>

Notes

The authors declare no competing financial interest.

ACKNOWLEDGMENTS

The authors thank Zhejiang Provincial Natural Science Foundation of China (grant no. LR22D010001 to F.J.), China Postdoctoral Science Foundation (2022M712842 to X.Z.), and the Key R&D Program of Zhejiang (grant no. 2022C03075 to F.J.) for financial support. We acknowledge the Westlake University HPC Center for computational support.

REFERENCES

- (1) Tsapekos, P.; Khoshnevisan, B.; Alvarado-Morales, M.; Zhu, X.; Pan, J.; Tian, H.; Angelidaki, I. Upcycling the Anaerobic Digestion Streams in a Bioeconomy Approach: A Review. *Renewable Sustainable Energy Rev.* **2021**, *151*, 111635.
- (2) Zhu, Y.-G.; Johnson, T. A.; Su, J.-Q.; Qiao, M.; Guo, G.-X.; Stedtfeld, R. D.; Hashsham, S. A.; Tiedje, J. M. Diverse and Abundant Antibiotic Resistance Genes in Chinese Swine Farms. *Proc. Natl. Acad. Sci. U.S.A.* **2013**, *110* (9), 3435–3440.
- (3) Ju, F.; Li, B.; Ma, L.; Wang, Y.; Huang, D.; Zhang, T. Antibiotic Resistance Genes and Human Bacterial Pathogens: Co-Occurrence, Removal, and Enrichment in Municipal Sewage Sludge Digesters. *Water Res.* **2016**, *91*, 1–10.
- (4) Wright, G. D. Environmental and Clinical Antibiotic Resistomes, Same Only Different. *Curr. Opin. Microbiol.* **2019**, *51*, 57–63.
- (5) Zhang, Z.; Zhang, Q.; Wang, T.; Xu, N.; Lu, T.; Hong, W.; Penuelas, J.; Gillings, M.; Wang, M.; Gao, W.; Qian, H. Assessment of Global Health Risk of Antibiotic Resistance Genes. *Nat. Commun.* **2022**, *13* (1), 1553.
- (6) Martinez, J. L. Antibiotics and Antibiotic Resistance Genes in Natural Environments. *Science* **2008**, *321* (5887), 365–367.
- (7) Anthony, W. E.; Wang, B.; Sukhum, K. V.; D'Souza, A. W.; Hink, T.; Cass, C.; Seiler, S.; Reske, K. A.; Coon, C.; Dubberke, E. R.; Burnham, C.-A. D.; Dantas, G.; Kwon, J. H. Acute and Persistent Effects of Commonly Used Antibiotics on the Gut Microbiome and Resistome in Healthy Adults. *Cell Rep.* **2022**, *39* (2), 110649.
- (8) Shuai, M.; Zhang, G.; Zeng, F.; Fu, Y.; Liang, X.; Yuan, L.; Xu, F.; Gou, W.; Miao, Z.; Jiang, Z.; Wang, J.; Zhuo, L.; Chen, Y.; Ju, F.; Zheng, J.-S. Human Gut Antibiotic Resistome and Progression of Diabetes. *Adv. Sci.* **2022**, *9* (11), 2104965.
- (9) Forsberg, K. J.; Patel, S.; Gibson, M. K.; Lauber, C. L.; Knight, R.; Fierer, N.; Dantas, G. Bacterial Phylogeny Structures Soil Resistomes across Habitats. *Nature* **2014**, *509* (7502), 612–616.
- (10) Zhang, Z.; Zhu, X.; Su, J.-Q.; Zhu, S.; Zhang, L.; Ju, F. Metagenomic Insights into Potential Impacts of Antibacterial Biosynthesis and Anthropogenic Activity on Nationwide Soil Resistome. *J. Hazard. Mater.* **2024**, *473*, 134677.
- (11) He, L.; Huang, X.; Zhang, G.; Yuan, L.; Shen, E.; Zhang, L.; Zhang, X.-H.; Zhang, T.; Tao, L.; Ju, F. Distinctive Signatures of Pathogenic and Antibiotic Resistant Potentials in the Hadal Microbiome. *Environ. Microbiome* **2022**, *17* (1), 19.
- (12) Zhang, Q.; Zhang, Z.; Lu, T.; Peijnenburg, W.; Gillings, M.; Yang, X.; Chen, J.; Penuelas, J.; Zhu, Y.-G.; Zhou, N.-Y.; et al. Cyanobacterial Blooms Contribute to the Diversity of Antibiotic-Resistance Genes in Aquatic Ecosystems. *Commun. Biol.* **2020**, *3* (1), 737.
- (13) Danko, D.; Bezdán, D.; Afshin, E. E.; Ahsanuddin, S.; Bhattacharya, C.; Butler, D. J.; Chng, K. R.; Donnellan, D.; Hecht, J.; Jackson, K.; et al. A Global Metagenomic Map of Urban Microbiomes and Antimicrobial Resistance. *Cell* **2021**, *184* (13), 3376–3393.e17.
- (14) Guo, J.; Li, J.; Chen, H.; Bond, P. L.; Yuan, Z. Metagenomic Analysis Reveals Wastewater Treatment Plants as Hotspots of Antibiotic Resistance Genes and Mobile Genetic Elements. *Water Res.* **2017**, *123*, 468–478.
- (15) Ju, F.; Beck, K.; Yin, X.; Maccagnan, A.; McArdell, C. S.; Singer, H. P.; Johnson, D. R.; Zhang, T.; Bürgmann, H. Wastewater Treatment Plant Resistomes Are Shaped by Bacterial Composition, Genetic Exchange, and Upregulated Expression in the Effluent Microbiomes. *ISME J.* **2019**, *13* (2), 346–360.
- (16) Zarei-Baygi, A.; Harb, M.; Wang, P.; Stadler, L. B.; Smith, A. L. Evaluating Antibiotic Resistance Gene Correlations with Antibiotic Exposure Conditions in Anaerobic Membrane Bioreactors. *Environ. Sci. Technol.* **2019**, *53* (7), 3599–3609.
- (17) Mazzurco Miritana, V.; Massini, G.; Visca, A.; Grenni, P.; Patrolecco, L.; Spataro, F.; Rauseo, J.; Garbini, G. L.; Signorini, A.; Rosa, S.; Barra Caracciolo, A. Effects of Sulfamethoxazole on the Microbial Community Dynamics During the Anaerobic Digestion Process. *Front. Microbiol.* **2020**, *11*, 537783.
- (18) Su, Y.; Wang, J.; Xia, H.; Xie, B.; Li, X. Anaerobic/Aerobic Conditions Determine Antibiotic Resistance Genes Removal Patterns from Leachate by Affecting Bacteria Taxa-Genes Co-Occurrence Modules. *Chemosphere* **2019**, *223*, 28–38.
- (19) Xia, X.; Wang, Z.; Fu, Y.; Du, X.; Gao, B.; Zhou, Y.; He, J.; Wang, Y.; Shen, J.; Jiang, H.; Wu, Y. Association of Colistin Residues and Manure Treatment with the Abundance of Mcr-1 Gene in Swine Feedlots. *Environ. Int.* **2019**, *127*, 361–370.
- (20) Zou, Y.; Xiao, Y.; Wang, H.; Fang, T.; Dong, P. New Insight into Fates of Sulfonamide and Tetracycline Resistance Genes and Resistant Bacteria during Anaerobic Digestion of Manure at Thermophilic and Mesophilic Temperatures. *J. Hazard. Mater.* **2020**, *384*, 121433.
- (21) Yun, H.; Liang, B.; Ding, Y.; Li, S.; Wang, Z.; Khan, A.; Zhang, P.; Zhang, P.; Zhou, A.; Wang, A.; Li, X. Fate of Antibiotic Resistance Genes during Temperature-Changed Psychrophilic Anaerobic Digestion of Municipal Sludge. *Water Res.* **2021**, *194*, 116926.
- (22) Zhang, J.; Lu, T.; Shen, P.; Sui, Q.; Zhong, H.; Liu, J.; Tong, J.; Wei, Y. The Role of Substrate Types and Substrate Microbial Community on the Fate of Antibiotic Resistance Genes during Anaerobic Digestion. *Chemosphere* **2019**, *229*, 461–470.
- (23) Zhang, Z.; Li, X.; Liu, H.; Gao, L.; Wang, Q. Free Ammonia Pretreatment Enhances the Removal of Antibiotic Resistance Genes in Anaerobic Sludge Digestion. *Chemosphere* **2021**, *279*, 130910.
- (24) Wang, G.; Chu, Y.; Zhu, J.; Sheng, L.; Liu, G.; Xing, Y.; Fu, P.; Li, Q.; Chen, R. Multi-Faceted Influences of Biochar Addition on Swine Manure Digestion under Tetracycline Antibiotic Pressure. *Bioresour. Technol.* **2022**, *346*, 126352.
- (25) Xu, S.; Duan, Y.; Zou, S.; Liu, H.; Luo, L.; Wong, J. W. C. Evaluations of Biochar Amendment on Anaerobic Co-Digestion of Pig Manure and Sewage Sludge: Waste-to-Methane Conversion, Microbial Community, and Antibiotic Resistance Genes. *Bioresour. Technol.* **2022**, *346*, 126400.
- (26) Zhang, R.; Gu, J.; Wang, X.; Li, Y. Antibiotic Resistance Gene Transfer during Anaerobic Digestion with Added Copper: Important Roles of Mobile Genetic Elements. *Sci. Total Environ.* **2020**, *743*, 140759.
- (27) Zhang, J.; Lu, T.; Zhong, H.; Shen, P.; Wei, Y. Zero Valent Iron Improved Methane Production and Specifically Reduced Amino-glycoside and Tetracycline Resistance Genes in Anaerobic Digestion. *Waste Manage.* **2021**, *136*, 122–131.
- (28) Zhang, Y.; Yang, Z.; Xiang, Y.; Xu, R.; Zheng, Y.; Lu, Y.; Jia, M.; Sun, S.; Cao, J.; Xiong, W. Evolutions of Antibiotic Resistance Genes (ARGs), Class 1 Integron-Integrase (intI1) and Potential Hosts of ARGs during Sludge Anaerobic Digestion with the Iron Nanoparticles Addition. *Sci. Total Environ.* **2020**, *724*, 138248.
- (29) Zhang, L.; Loh, K.-C.; Zhang, J. Jointly Reducing Antibiotic Resistance Genes and Improving Methane Yield in Anaerobic Digestion of Chicken Manure by Feedstock Microwave Pretreatment

- and Activated Carbon Supplementation. *Chem. Eng. J.* **2019**, *372*, 815–824.
- (30) United Nations Environment Programme. *Environmental Dimensions of Antimicrobial Resistance*; United Nations Environment Programme, 2022.
- (31) Dai, D.; Brown, C.; Bürgmann, H.; Larsson, D. G. J.; Nambi, I.; Zhang, T.; Flach, C.-F.; Pruden, A.; Vikesland, P. J. Long-Read Metagenomic Sequencing Reveals Shifts in Associations of Antibiotic Resistance Genes with Mobile Genetic Elements from Sewage to Activated Sludge. *Microbiome* **2022**, *10* (1), 20.
- (32) Zhang, Z.; Zhang, G.; Ju, F. Using Culture-Enriched Phenotypic Metagenomics for Targeted High-Throughput Monitoring of the Clinically Important Fraction of the β -Lactam Resistome. *Environ. Sci. Technol.* **2022**, *56* (16), 11429–11439.
- (33) Boolchandani, M.; D'Souza, A. W.; Dantas, G. Sequencing-Based Methods and Resources to Study Antimicrobial Resistance. *Nat. Rev. Genet.* **2019**, *20* (6), 356–370.
- (34) Yuan, L.; Wang, Y.; Zhang, L.; Palomo, A.; Zhou, J.; Smets, B. F.; Bürgmann, H.; Ju, F. Pathogenic and Indigenous Denitrifying Bacteria Are Transcriptionally Active and Key Multi-Antibiotic-Resistant Players in Wastewater Treatment Plants. *Environ. Sci. Technol.* **2021**, *55* (15), 10862–10874.
- (35) Alcock, B. P.; Huynh, W.; Chalil, R.; Smith, K. W.; Raphenya, A. R.; Wlodarski, M. A.; Edalatmand, A.; Petkau, A.; Syed, S. A.; Tsang, K. K.; Baker, S. J. C.; Dave, M.; McCarthy, M. C.; Mukiri, K. M.; Nasir, J. A.; Golbon, B.; Imtiaz, H.; Jiang, X.; Kaur, K.; Kwong, M.; Liang, Z. C.; Niu, K. C.; Shan, P.; Yang, J. Y. J.; Gray, K. L.; Hoad, G. R.; Jia, B.; Bhando, T.; Carfrae, L. A.; Farha, M. A.; French, S.; Gordzevich, R.; Rachwalski, K.; Tu, M. M.; Bordeleau, E.; Dooley, D.; Griffiths, E.; Zubyk, H. L.; Brown, E. D.; Maguire, F.; Beiko, R. G.; Hsiao, W. W. L.; Brinkman, F. S. L.; Van Domselaar, G.; McArthur, A. G. CARD 2023: Expanded Curation, Support for Machine Learning, and Resistome Prediction at the Comprehensive Antibiotic Resistance Database. *Nucleic Acids Res.* **2023**, *51* (D1), D690–D699.
- (36) Yin, X.; Zheng, X.; Li, L.; Zhang, A.-N.; Jiang, X.-T.; Zhang, T. ARGs-OAP v3.0: Antibiotic-Resistance Gene Database Curation and Analysis Pipeline Optimization. *Engineering* **2023**, *27*, 234–241.
- (37) Ju, F.; Zhang, T. Experimental Design and Bioinformatics Analysis for the Application of Metagenomics in Environmental Sciences and Biotechnology. *Environ. Sci. Technol.* **2015**, *49* (21), 12628–12640.
- (38) Ma, S.; Jiang, F.; Huang, Y.; Zhang, Y.; Wang, S.; Fan, H.; Liu, B.; Li, Q.; Yin, L.; Wang, H.; Liu, H.; Ren, Y.; Li, S.; Cheng, L.; Fan, W.; Deng, Y. A Microbial Gene Catalog of Anaerobic Digestion from Full-Scale Biogas Plants. *GigaScience* **2021**, *10* (1), g1aa164.
- (39) Frank, J. A.; Pan, Y.; Tooming-Klunderud, A.; Eijssink, V. G. H.; McHardy, A. C.; Nederbragt, A. J.; Pope, P. B. Improved Metagenome Assemblies and Taxonomic Binning Using Long-Read Circular Consensus Sequence Data. *Sci. Rep.* **2016**, *6* (1), 25373.
- (40) Hao, L.; Michaelsen, T. Y.; Singleton, C. M.; Dottorini, G.; Kirkegaard, R. H.; Albertsen, M.; Nielsen, P. H.; Dueholm, M. S. Novel Syntrophic Bacteria in Full-Scale Anaerobic Digesters Revealed by Genome-Centric Metatranscriptomics. *ISME J.* **2020**, *14* (4), 906–918.
- (41) Jonassen, K. R.; Hagen, L. H.; Vick, S. H. W.; Arntzen, M. Ø.; Eijssink, V. G. H.; Frostegård, Å.; Lycus, P.; Molstad, L.; Pope, P. B.; Bakken, L. R. Nitrous Oxide Respiring Bacteria in Biogas Digestates for Reduced Agricultural Emissions. *ISME J.* **2022**, *16* (2), 580–590.
- (42) Luo, G.; Li, B.; Li, L.-G.; Zhang, T.; Angelidaki, I. Antibiotic Resistance Genes and Correlations with Microbial Community and Metal Resistance Genes in Full-Scale Biogas Reactors As Revealed by Metagenomic Analysis. *Environ. Sci. Technol.* **2017**, *51* (7), 4069–4080.
- (43) Ruiz-Sánchez, J.; Campanaro, S.; Guivernau, M.; Fernández, B.; Prenafeta-Boldú, F. Effect of Ammonia on the Active Microbiome and Metagenome from Stable Full-Scale Digesters. *Bioresour. Technol.* **2018**, *250*, 513–522.
- (44) Stolze, Y.; Bremges, A.; Rummig, M.; Henke, C.; Maus, I.; Pühler, A.; Sczyrba, A.; Schlüter, A. Identification and Genome Reconstruction of Abundant Distinct Taxa in Microbiomes from One Thermophilic and Three Mesophilic Production-Scale Biogas Plants. *Biotechnol. Biofuels* **2016**, *9* (1), 156.
- (45) Maus, I.; Koeck, D. E.; Cibis, K. G.; Hahnke, S.; Kim, Y. S.; Langer, T.; Kreubel, J.; Erhard, M.; Bremges, A.; Off, S.; Stolze, Y.; Jaenicke, S.; Goesmann, A.; Sczyrba, A.; Scherer, P.; König, H.; Schwarz, W. H.; Zverlov, V. V.; Liebl, W.; Pühler, A.; Schlüter, A.; Klocke, M. Unraveling the Microbiome of a Thermophilic Biogas Plant by Metagenome and Metatranscriptome Analysis Completed by Characterization of Bacterial and Archaeal Isolates. *Biotechnol. Biofuels* **2016**, *9* (1), 171.
- (46) Bremges, A.; Maus, I.; Belmann, P.; Eikmeyer, F.; Winkler, A.; Albersmeier, A.; Pühler, A.; Schlüter, A.; Sczyrba, A. Deeply Sequenced Metagenome and Metatranscriptome of a Biogas-Producing Microbial Community from an Agricultural Production-Scale Biogas Plant. *GigaScience* **2015**, *4* (1), 33.
- (47) Bolger, A. M.; Lohse, M.; Usadel, B. Trimmomatic: A Flexible Trimmer for Illumina Sequence Data. *Bioinformatics* **2014**, *30* (15), 2114–2120.
- (48) Wood, D. E.; Lu, J.; Langmead, B. Improved Metagenomic Analysis with Kraken 2. *Genome Biol.* **2019**, *20* (1), 257.
- (49) Yin, X.; Chen, X.; Jiang, X.-T.; Yang, Y.; Li, B.; Shum, M. H.-H.; Lam, T. T. Y.; Leung, G. M.; Rose, J.; Sanchez-Cid, C.; Vogel, T. M.; Walsh, F.; Berendonk, T. U.; Midega, J.; Uchea, C.; Frigon, D.; Wright, G. D.; Bezuidenhout, C.; Picão, R. C.; Ahammad, S. Z.; Nielsen, P. H.; Hugenholtz, P.; Ashbolt, N. J.; Corno, G.; Fatta-Kassinos, D.; Bürgmann, H.; Schmitt, H.; Cha, C.-J.; Pruden, A.; Smalla, K.; Cytryn, E.; Zhang, Y.; Yang, M.; Zhu, Y.-G.; Dechesne, A.; Smets, B. F.; Graham, D. W.; Gillings, M. R.; Gaze, W. H.; Manaia, C. M.; Van Loosdrecht, M. C. M.; Alvarez, P. J. J.; Blaser, M. J.; Tiedje, J. M.; Topp, E.; Zhang, T. Toward a Universal Unit for Quantification of Antibiotic Resistance Genes in Environmental Samples. *Environ. Sci. Technol.* **2023**, *57*, 9713–9721.
- (50) Zhang, A.-N.; Gaston, J. M.; Dai, C. L.; Zhao, S.; Poyet, M.; Groussin, M.; Yin, X.; Li, L.-G.; van Loosdrecht, M.; Topp, E.; et al. An Omics-Based Framework for Assessing the Health Risk of Antimicrobial Resistance Genes. *Nat. Commun.* **2021**, *12* (1), 4765.
- (51) Li, B.; Yang, Y.; Ma, L.; Ju, F.; Guo, F.; Tiedje, J. M.; Zhang, T. Metagenomic and Network Analysis Reveal Wide Distribution and Co-Occurrence of Environmental Antibiotic Resistance Genes. *ISME J.* **2015**, *9* (11), 2490–2502.
- (52) Ju, F.; Xia, Y.; Guo, F.; Wang, Z.; Zhang, T. Taxonomic Relatedness Shapes Bacterial Assembly in Activated Sludge of Globally Distributed Wastewater Treatment Plants. *Environ. Microbiol.* **2014**, *16* (8), 2421–2432.
- (53) Dixon, P. VEGAN, a Package of R Functions for Community Ecology. *J. Veg. Sci.* **2003**, *14* (6), 927–930.
- (54) Csardi, G.; Nepusz, T. The Igraph Software Package for Complex Network Research. *Interjunct* **2006**, *1695* (5), 1–9.
- (55) Harrell, F. E., Jr.; Harrell, M. F. E., Jr. Package 'Hmisc'. CRAN2018, 2019, pp 235–236.
- (56) Bastian, M.; Heymann, S.; Jacomy, M. Gephi: An Open Source Software for Exploring and Manipulating Networks. *Proceedings of the international AAAI conference on web and social media*, 2009; Vol. 3; pp 361–362.
- (57) Nurk, S.; Meleshko, D.; Korobeynikov, A.; Pevzner, P. A. metaSPAdes: A New Versatile Metagenomic Assembler. *Genome Res.* **2017**, *27* (5), 824–834.
- (58) Camargo, A. P.; Roux, S.; Schulz, F.; Babinski, M.; Xu, Y.; Hu, B.; Chain, P. S. G.; Nayfach, S.; Kyrpides, N. C. Identification of Mobile Genetic Elements with geNomad. *Nat. Biotechnol.* **2023**, *42*, 1303–1312.
- (59) Nayfach, S.; Camargo, A. P.; Schulz, F.; Eloie-Fadrosch, E.; Roux, S.; Kyrpides, N. C. CheckV Assesses the Quality and Completeness of Metagenome-Assembled Viral Genomes. *Nat. Biotechnol.* **2021**, *39* (5), 578–585.
- (60) Bushnell, B. BBMap: A Fast, Accurate, Splice-Aware Aligner; LBNL-7065E; Lawrence Berkeley National Lab. (LBNL): Berkeley,

CA, 2014. <https://www.osti.gov/biblio/1241166> (accessed 16 November 2022).

(61) Oh, M.; Pruden, A.; Chen, C.; Heath, L. S.; Xia, K.; Zhang, L. MetaCompare: A Computational Pipeline for Prioritizing Environmental Resistome Risk. *FEMS Microbiol. Ecol.* **2018**, *94* (7), fty079.

(62) Kang, D. D.; Li, F.; Kirton, E.; Thomas, A.; Egan, R.; An, H.; Wang, Z. MetaBAT 2: An Adaptive Binning Algorithm for Robust and Efficient Genome Reconstruction from Metagenome Assemblies. *PeerJ* **2019**, *7*, No. e7359.

(63) Olm, M. R.; Brown, C. T.; Brooks, B.; Banfield, J. F. dRep: A Tool for Fast and Accurate Genomic Comparisons That Enables Improved Genome Recovery from Metagenomes through de-Replication. *ISME J.* **2017**, *11* (12), 2864–2868.

(64) Parks, D. H.; Imelfort, M.; Skennerton, C. T.; Hugenholtz, P.; Tyson, G. W. C.M. CheckM: assessing the quality of microbial genomes recovered from isolates, single cells, and metagenomes. *Genome Res.* **2015**, *25* (7), 1043–1055.

(65) Chaumeil, P.-A.; Mussig, A. J.; Hugenholtz, P.; Parks, D. H. GTDB-Tk: A Toolkit to Classify Genomes with the Genome Taxonomy Database. *Bioinformatics* **2019**, *36*, 1925–1927.

(66) Bosi, E.; Donati, B.; Galardini, M.; Brunetti, S.; Sagot, M.-F.; Lió, P.; Crescenzi, P.; Fani, R.; Fondi, M. MeDuSa: A Multi-Draft Based Scaffold. *Bioinformatics* **2015**, *31* (15), 2443–2451.

(67) Cantalapiedra, C. P.; Hernández-Plaza, A.; Letunic, I.; Bork, P.; Huerta-Cepas, J. eggNOG-Mapper v2: Functional Annotation, Orthology Assignments, and Domain Prediction at the Metagenomic Scale. *Mol. Biol. Evol.* **2021**, *38* (12), 5825–5829.

(68) Bowers, R. M.; Kyrpides, N. C.; Stepanauskas, R.; Harmon-Smith, M.; Doud, D.; Reddy, T. B. K.; Schulz, F.; Jarett, J.; Rivers, A. R.; Elie-Fadrosh, E. A.; Tringe, S. G.; Ivanova, N. N.; Copeland, A.; Clum, A.; Becraft, E. D.; Malmstrom, R. R.; Birren, B.; Podar, M.; Bork, P.; Weinstock, G. M.; Garrity, G. M.; Dodsworth, J. A.; Yooseph, S.; Sutton, G.; Glöckner, F. O.; Gilbert, J. A.; Nelson, W. C.; Hallam, S. J.; Jungbluth, S. P.; Ettema, T. J. G.; Tighe, S.; Konstantinidis, K. T.; Liu, W.-T.; Baker, B. J.; Rattei, T.; Eisen, J. A.; Hedlund, B.; McMahon, K. D.; Fierer, N.; Knight, R.; Finn, R.; Cochrane, G.; Karsch-Mizrachi, I.; Tyson, G. W.; Rinke, C.; Lapidus, A.; Meyer, F.; Yilmaz, P.; Parks, D. H.; Murat Eren, A.; Schriml, L.; Banfield, J. F.; Hugenholtz, P.; Woyke, T. Minimum Information about a Single Amplified Genome (MISAG) and a Metagenome-Assembled Genome (MIMAG) of Bacteria and Archaea. *Nat. Biotechnol.* **2017**, *35* (8), 725–731.

(69) Lee, H.; Hsu, F.-F.; Turk, J.; Groisman, E. A. The PmrA-Regulated pmrC Gene Mediates Phosphoethanolamine Modification of Lipid A and Polymyxin Resistance in *Salmonella Enterica*. *J. Bacteriol.* **2004**, *186*, 4124–4133.

(70) Hoffmann, F.; Rinas, U. Plasmid Amplification in *Escherichia Coli* after Temperature Upshift Is Impaired by Induction of Recombinant Protein Synthesis. *Biotechnol. Lett.* **2001**, *23* (22), 1819–1825.

(71) Brown, C. L.; Mullet, J.; Hindi, F.; Stoll, J. E.; Gupta, S.; Choi, M.; Keenum, I.; Vikesland, P.; Pruden, A.; Zhang, L. mobileOG-Db: A Manually Curated Database of Protein Families Mediating the Life Cycle of Bacterial Mobile Genetic Elements. *Appl. Environ. Microbiol.* **2022**, *88* (18), 009911–22.

(72) Tian, Z.; Zhang, Y.; Yu, B.; Yang, M. Changes of Resistome, Mobilome and Potential Hosts of Antibiotic Resistance Genes during the Transformation of Anaerobic Digestion from Mesophilic to Thermophilic. *Water Res.* **2016**, *98*, 261–269.

(73) Lin, M.; Ren, L.; Mondon Wandra, S.; Liu, Y.; Dong, R.; Qiao, W. Enhancing Pathogen Inactivation in Pig Manure by Introducing Thermophilic and Hyperthermophilic Hygienization in a Two-Stage Anaerobic Digestion Process. *Waste Manage.* **2022**, *144*, 123–131.

(74) Francis, D. M.; Page, R. Strategies to Optimize Protein Expression in *E. coli*. *Curr. Protoc. Protein Sci.* **2010**, *61* (1), 5.24.1–5.24.29.